

Do Models Underestimate the Solar Contribution to Recent Climate Change?

PETER A. STOTT, GARETH S. JONES, AND JOHN F. B. MITCHELL

Hadley Centre for Climate Prediction and Research, Met Office, Bracknell, Berkshire, United Kingdom

(Manuscript received 2 September 2002, in final form 10 June 2003)

ABSTRACT

Current attribution analyses that seek to determine the relative contributions of different forcing agents to observed near-surface temperature changes underestimate the importance of weak signals, such as that due to changes in solar irradiance. Here a new attribution method is applied that does not have a systematic bias against weak signals.

It is found that current climate models underestimate the observed climate response to solar forcing over the twentieth century as a whole, indicating that the climate system has a greater sensitivity to solar forcing than do models. The results from this research show that increases in solar irradiance are likely to have had a greater influence on global-mean temperatures in the first half of the twentieth century than the combined effects of changes in anthropogenic forcings. Nevertheless the results confirm previous analyses showing that greenhouse gas increases explain most of the global warming observed in the second half of the twentieth century.

1. Introduction

A number of recent studies have estimated the magnitude of large-scale temperature responses to various external influences over the twentieth century (e.g., Tett et al. 1999; Barnett et al. 1999; Allen et al. 2002; Tett et al. 2002). On the basis of such evidence the Third Assessment Report of the Intergovernmental Panel on Climate Change (IPCC) were able to conclude that “most of the observed warming over the last 50 years is likely to have been due to the increase in greenhouse gas concentrations” (Mitchell et al. 2001). Quantifying the contributions of anthropogenic and natural factors to past climate change also allows constraints to be placed on predictions of future climate change (Allen et al. 2000; Stott and Kettleborough 2002).

Most of the warming of the twentieth century occurred during two distinct periods, from about 1910 to the mid-1940s and from the mid-1970s. Greenhouse gases provide the largest increases in climate forcing during the twentieth century and would therefore be expected to have contributed most to observed warming if the climate sensitivity is similar for different forcings. However, other forcing agents have also influenced past climate change.

Coupled model simulations indicate that the global warming trend observed in the latter part of the twentieth century is inconsistent with simulations that omit

observed increases in greenhouse gases (Stott et al. 2000; Cubasch et al. 1997). Coupled model simulations including anthropogenic forcings show that warming over the last 50 yr can be explained by a combination of greenhouse warming balanced by cooling from sulfate aerosols (Stott et al. 2000; Delworth and Knutson 2000; Dai et al. 2001) but these simulations generally fail to simulate the overall temporal evolution of twentieth-century global temperature.

Multidecadal variability associated with the thermohaline circulation could have contributed to global warming observed before 1950 (Delworth and Knutson 2000), but this was also a period in which forcing from natural external factors is likely to have been positive. Between the eruptions of Katmai in 1912 and Agung in 1963 there was relatively little volcanic activity capable of releasing aerosols into the stratosphere (Sato et al. 1993). A number of reconstructions of solar irradiance based on sunspot data estimate that there was a general increase in solar forcing in the first half of the twentieth century overlying the 11-yr solar cycle (Lean 2000; Hoyt and Schatten 1993; Solanki and Fligge 2002). Climate model simulations that include volcanic aerosol and estimated changes in solar irradiance in addition to anthropogenic forcings provide a more consistent explanation of temperature changes throughout the twentieth century than simulations that omit the natural forcings (Stott et al. 2000).

Based on comparisons between simple climate model simulations and reconstructions of Northern Hemisphere temperature changes since 1000, Crowley (2000) showed that a large part of the decadal-scale temperature

Corresponding author address: Dr. Peter A. Stott, Hadley Centre for Climate Prediction and Research, Met Office, London Road, Bracknell, Berkshire RG12 2SY, United Kingdom.
E-mail: peter.stott@metoffice.com

variability in preindustrial climate could be explained by changes in solar irradiance and volcanism. A simulation including just solar irradiance changes alone (Rind 2002) indicates that in some periods (such as the eighteenth century) solar forcing was more likely to be important whereas in other periods (such as the nineteenth century) volcanism probably played a greater role, although another study indicates that volcanic forcing was generally dominant (Hegerl et al. 2003).

Satellite measurement of solar irradiance have only been made since 1978 and show a clear 11-yr cycle with variations in total irradiance of approximately 0.1%, although there are much higher variations in the ultraviolet (UV) of around 10% near 200 nm and 4% near 300 nm (Larkin et al. 2000). Reconstructions before the satellite record are based on proxy data, most notably sunspot measurements. When the overall increase since the Maunder minimum of solar activity is constrained to observations of sunlike stars (Lean et al. 1995a; Lean 2000), it is estimated that there was approximately a 2 W m^{-2} increase in solar irradiance between 1900 and 1950, one of the most sustained periods of secular increase in solar irradiance since the Maunder minimum in the seventeenth century. This would have produced a radiative forcing of 0.35 W m^{-2} ($2 \times 0.7/4$ where the factor 0.7 accounts for the albedo of the earth and the factor 4 is the spherical average), comparable in magnitude to the greenhouse gas forcing over that period.

Reconstructions of solar irradiance are uncertain and based on differing assumptions about how solar observations can be used as proxies for long-term solar irradiance variations. They are supported by observations of the aa geomagnetic activity index (Lockwood et al. 1999) and of the cosmogenic isotopes ^{10}Be and ^{14}C that show an inverse correlation with reconstructions of solar irradiance, as would be expected if increasing solar activity is coupled with increases in the interplanetary magnetic field that shields the earth from cosmic rays. Although a variety of reconstructions employing different assumptions (Lean 2000; Hoyt and Schatten 1993; Solanki and Fligge 2002) all show long-term secular changes in solar irradiance, a recent solar model indicates that solar irradiance might be decoupled from the interplanetary magnetic field and that total solar irradiance might have increased very little since the Maunder minimum (Lean et al. 2002).

Correlations between variations in solar irradiance and climate variables have led to speculations that the relatively small direct forcing from solar variability could be amplified within the climate system. Solar ultraviolet irradiance variations affect stratospheric ozone, which can influence the troposphere via modulation of planetary waves (Shindell et al. 1999b) or modulation of the Hadley circulation (Haigh 1996). Another suggestion is that interactions between cosmic rays and clouds could amplify solar forcing (Marsh and Svensmark 2000). The cosmic ray intensity declined during the twentieth century as the interplanetary magnetic

field increased (Carslaw et al. 2002) and it has been postulated that global temperatures could be affected via changes in cloud formation processes (Yu 2002) or changes in the atmospheric potential gradient (Harrison 2002).

A recent study used the third Hadley Centre Coupled Ocean–Atmosphere General Circulation Model (HadCM3; Gordon et al. 2000; Pope et al. 2000) to estimate natural and anthropogenic contributions to twentieth-century temperature change (Tett et al. 2002). The model-simulated climatic responses to greenhouse gases, tropospheric aerosols, and ozone changes, and the combined response to solar irradiance changes and stratospheric volcanic aerosols were compared with observations using optimal detection (Hasselmann 1993), a form of linear regression (Allen and Tett 1999). Warming due to greenhouse gases was found to play a smaller part in the early twentieth-century warming than the later warming, which was found to be almost entirely caused by greenhouse gases, with tropospheric sulfate aerosols and natural factors (presumed to be stratospheric aerosols from volcanic eruptions) offsetting approximately one-third of the warming.

No evidence was found by Tett et al. (2002) that the model systematically underestimated the observed climatic response, as would be expected for solar forcing, if as discussed above, an amplifying mechanism were operative in the real world but not present in the model. However the analysis only considered runs of HadCM3 in which solar and volcanic forcings were included together, preventing separation of the model's response to these two forcings. In addition, the standard optimal detection methodology, which was applied by Tett et al. (2002), is known to have a bias that results in an underestimate of the magnitude of the climate response attributed to weak forcings when estimated by small ensembles of model simulations (Stott et al. 2003).

In section 2 we discuss a new regression technique that takes account of sampling noise in model-simulated response patterns and show that it makes the most difference to attribution of the natural contribution to observed twentieth-century temperature change. In section 3 we analyze two HadCM3 simulations, one including solar forcing and one including volcanic forcing, in addition to the anthropogenic simulations considered by Tett et al. (2002). Rather than make ensembles of runs, as was done previously to reduce noise contamination of the signal from natural internal variability, here we choose to amplify the solar and volcanic forcing input to the model and make a single simulation for each forcing. For our regression analysis, we require that the large-scale temperature response to a particular forcing scales linearly as the forcing is amplified. In section 3 we show that this linearity assumption is justified. Linearity then allows us to estimate the contributions to observed large-scale temperature changes from (unamplified) solar and volcanic forcings in addition to anthropogenic forcings. A feature of the technique is

that we can test for consistency between the observations and the model to determine if the model significantly underestimates the observed response to a particular (unamplified) forcing. In section 4 we present conclusions and a discussion of the implications for the debate on whether atmospheric processes could cause a larger climatic response than expected from the relatively small change in solar output estimated over the twentieth century.

2. Natural contributions to twentieth-century temperature change

The climate response to different forcing agents has been estimated by Stott et al. (2000) and Tett et al. (2002) using a variety of HadCM3 simulations. All HadCM3 runs including external forcing factors were initialized for 1 December 1859 (the model year starting on 1 December) from a 1830-yr control run of HadCM3 in which external forcings were held constant to represent internal variability. Members of multimember ensembles were initialized from different states of the control run separated by 100 yr. All analyses described in this paper are for the 100-yr period starting on 1 December 1899 (denoted 1900–99 for convenience).

The simulations are as follows:

- GHG: Ensemble of four runs forced with historical changes in well-mixed greenhouse gases.
- ANTHRO: Ensemble of four runs including both well-mixed greenhouse gases and anthropogenic sulfur emissions and their implied changes to cloud albedos, as well as tropospheric and stratospheric ozone changes.
- NATURAL: Ensemble of four runs forced with changes in stratospheric aerosol following volcanic eruptions, according to the updated reconstruction of Sato et al. (1993), and changes in solar irradiance, according to the updated reconstruction of Lean et al. (1995a), including a greater variation in UV than total irradiance.
- ALL: Ensemble of four runs including all the forcings included in ANTHRO and NATURAL.

Our aim is to include the most important forcings over the twentieth century but we have omitted land use changes and forcing from black carbon emissions. Although these two climate forcings are estimated to be relatively small (Houghton et al. 2001), further investigation is required to determine whether they could contribute significantly to twentieth-century climate change. Further details of the simulations are given in appendix A and a comprehensive description can be found in Tett et al. (2002) and Johns et al. (2003). The observational dataset we use is an updated version of the combined dataset of 1.5-m air temperature over land and sea surface temperatures of Parker et al. (1994).

The methodology applied here, as in Tett et al. (2002), is to express observed decadal-mean near-surface tem-

perature changes over the twentieth century, \mathbf{y} , as a linear sum of simulated changes from various forcing agents, such as the three signals described above: \mathbf{x}_1 (GHG), \mathbf{x}_2 (ANTHRO), and \mathbf{x}_3 (NATURAL). The observations, \mathbf{y} , and each model signal, \mathbf{x}_i , are vectors that contain anomalous near-surface temperature data at each point in space and time, where the data are masked and filtered spatially and temporally, as described below. The methodology we apply differs from that applied by Tett et al. (2002) in assuming a different statistical model of the relationship between model-simulated signals and the observed record. Tett et al. (2002) assumed that the observations, \mathbf{y} , can be represented as a linear superposition of m model-simulated response patterns, \mathbf{x}_i , multiplied by unknown scaling factors, β_i , to be estimated in the regression, plus an additive noise term, \mathbf{u}_0 :

$$\mathbf{y} = \sum_{i=1}^m \mathbf{x}_i \beta_i + \mathbf{u}_0. \quad (1)$$

However model-simulated response patterns are contaminated by noise from natural internal variability. This can be reduced by making ensembles of simulations, each starting from different initial conditions, and averaging them. Nevertheless contamination by noise remains; the model-simulated patterns are different from the “true” model patterns of response that would be obtained from averaging an infinitely large ensemble of simulations. Here we apply total least squares (TLS) regression, which takes into account the fact that the model-simulated responses from a finite ensemble, \mathbf{x}_i , must differ from the underlying noise-free response that would be obtained from a hypothetical infinite ensemble. An additional noise term, \mathbf{u}_i , is included in the expression, and the observations are represented more accurately by

$$\mathbf{y} = \sum_{i=1}^m (\mathbf{x}_i - \mathbf{u}_i) \beta_i + \mathbf{u}_0. \quad (2)$$

For ease of discussion, we now consider the case in which there is a single model-simulated signal, \mathbf{x} , and the regression is carried out in two dimensions, but the argument generalizes to multiple signals and regression in three or more dimensions. By taking account of uncertainty both in \mathbf{x} and \mathbf{y} , TLS minimizes the distance perpendicular to the best-fit line. In contrast, standard regression [applied by Tett et al. (2002)] assumes no uncertainty in \mathbf{x} and therefore minimizes the vertical distance between the scatter of points and the best-fit line. If measurements of both \mathbf{x} and \mathbf{y} are subject to uncertainty, the line obtained by minimizing the vertical distance has a smaller slope than the correct estimate of the best-fit line, obtained by minimizing the perpendicular distance. In consequence, β is underestimated by standard regression; Stott et al. (2003) showed that this is most serious for small ensembles of weak signals.

The solution of Eq. (2) in the case of multiple signals was demonstrated by Allen and Stott (2003) who gen-

TABLE 1. Best estimates of scaling factors, β_i , for analyses of the 1900–99 period (with the 5th–95th percentile uncertainty range shown in parentheses) using decadally averaged data.

	G	SO	NATURAL
Standard regression vs OBS	0.90 (0.66–1.15)	0.61 (0.16–1.07)	0.91 (0.38–1.44)
TLS regression vs OBS	1.07 (0.76–1.46)	0.98 (0.36–1.77)	1.65 (0.95–2.72)
TLS regression vs ALL	0.82 (0.58–1.10)	0.73 (0.26–1.28)	1.12 (0.57–1.83)

eralized Ripley and Thompson's (1987) approach, based on maximum likelihood fitting of a functional relationship. Stott et al. (2003) demonstrated that TLS regression, when applied to signals generated by the HadCM2 coupled climate model in a perfect model experiment, showed no systematic bias. A brief summary of the TLS methodology is given in appendix B.

Here we consider decadal-mean data for the 1900–99 period that are masked by the observational data mask and smoothed spatially to retain only scales greater than 5000 km (Stott and Tett 1998). Although the regression method is different, and a different time period is chosen (1900–99 rather than 1898–1997), the other important aspects of the methodology are the same as that described by Tett et al. (2002), and further details are given in appendix A. Estimates of the scaling factors, β_i , and their uncertainties, require estimates of the covariance matrix of internal variability that are obtained either from the control run or from intraensemble differences (see appendix B). Because we do not have enough data to estimate accurately the inverse of the covariance matrix [required for the solution of Eqs. (1) and (2)], the standard procedure applied here is to estimate its inverse from a truncated representation based on its leading eigenvectors. Here we truncate model and observed data to the leading 24 eigenvectors, which represent the highest variance spatiotemporal modes of variability.

From the runs available, (GHG and ANTHRO), we wish to extract the pure greenhouse component (denoted G) and the nongreenhouse sulfate and ozone components (SO). Assuming that the climate response to these two different forcings is linearly additive (Haywood et al. 1997), it is possible to calculate the scaling factors on G and SO (see appendix C).

Table 1 shows the scaling factors, β_i , for the three components, G, SO, and NATURAL, calculated using standard regression and TLS regression over the period 1900–99. If the 5th–95th percentile uncertainty range includes 1, this indicates that the model simulation of this forcing is consistent with the estimated observed response. Where the 5th–95th percentile uncertainty range does not include 0, this indicates that the relevant signal has been detected at the 5% significance level (i.e., there is less than a 5% chance that natural variability rather than the forcing is responsible for the observed change).

We find that all three signals are detected at the 5% significance level with scaling factors all consistent with 1, whichever regression scheme is used (Table 1), the

results for standard regression being close to those found by Tett et al. (2002) for the 1898–1997 period. Scaling factors are all greater when calculated by TLS regression, illustrating how sampling noise results in a low bias for scaling factors calculated using standard regression (Table 1). The effect is relatively small for G and largest for NATURAL, which, over the twentieth century as a whole, has the smallest signal-to-noise ratio of the three signals [signal-to-noise ratios are 7.5, 3.2, 1.6 for G, SO, NATURAL, respectively, when they are calculated in the same way as in Tett et al. (2002)]. Although the scaling factors for all three signals are still consistent with 1, the 5th–95th percentile uncertainty range for the NATURAL signal is predominantly greater than 1 with a best estimate of 1.65 and an uncertainty range from 0.95 to 2.72.

The larger scaling factors for NATURAL compared to G and SO do not imply more warming from natural forcings than anthropogenic forcings over the twentieth century. The natural runs warm slightly (circa 0.1 K) during the first half of the century and cool (circa 0.1 K) during the second half of the century due to stratospheric aerosols from the eruptions of Agung in 1963, El Chichón in 1982, and Mt. Pinatubo in 1991. Amplifying factors from 0.95 to 2.72 imply warming in the first half of the century and cooling in the second half of the century between approximately 0.1 and 0.25 K, relatively small compared to warming from greenhouse gases of approximately 1 K over the century.

Scaling factors greater than 1 indicate that the model's response needs to be amplified to be consistent with the estimated observed response to that forcing. Therefore these results show that the model could potentially be systematically underestimating the climate's response to natural forcings. However, the NATURAL runs include solar and volcanic changes together, two very different forcings whose climate response is mediated by different physical processes. We therefore need to consider the model's response to these two forcings separately in order to determine which climate response is being underestimated by the model.

3. Climatic impact of solar and volcanic forcings

To determine whether the model is underestimating the response to solar or to volcanic forcing we have made three further simulations of HadCM3. In these simulations, the forcings were enhanced in order to obtain a clear signal of the climate response from a single simulation. This avoided the use of multimember en-

sembles for these forcings; the climatic response from a single run with unamplified natural forcings would be heavily contaminated by noise, and although TLS regression would give unbiased results in this situation, uncertainty limits would be large (tending to unbounded uncertainty limits as noise dominates the signal).

The simulations we have made were all initialized for 1 December 1859 from the control run and are as follows:

- **10×LBB:** A single simulation forced by enhanced changes in the solar irradiance according to the reconstruction of Lean et al. (1995a) with changes spread over the solar spectrum following Lean et al. (1995b). The model includes the effects of ozone absorption on the spectral distribution of radiation. Solar irradiance changes were enhanced by a factor of 10, keeping the relative proportional changes constant across wave bands. We do not include changes in stratospheric ozone or clouds as a direct result of changes in solar irradiance.

Note that HadCM3, with 19 vertical levels, has a coarse representation of the lower stratosphere and extends only to 5 hPa (30 km). Consequently the model could represent poorly any planetary wave response to changes in stratospheric temperature profile as a result of changes in solar irradiance. It has been argued that a resolved stratosphere is necessary to realistically represent the Arctic Oscillation–North Atlantic Oscillation (AO–NAO) response to changes in greenhouse and solar forcings (Shindell et al. 1999a; Shindell et al. 1999b) although Gillett et al. (2002) found no increase in NAO sensitivity in HadSM3 (the same atmospheric model as in HadCM3 coupled to a thermodynamics “slab” ocean model) when its stratospheric resolution is increased and its upper boundary is raised to over 80 km.

- **10×HS:** A single run forced by changes in the solar irradiance according to the reconstruction of Hoyt and Schatten (1993), enhanced in the same way as 10×LBB.
- **5×VOL:** A single run forced by changes in stratospheric aerosol following volcanic eruptions, according to the updated reconstruction of Sato et al. (1993) with optical depths enhanced by a factor of 5.

All simulations were run from 1 December 1859 to 30 November 1999 except for HS which was run until 30 November 1996 due to lack of solar irradiance data for the reconstruction after this date. For the 10×HS simulation only, the decadal mean for the 1990s was constructed using the 6 yr of model data available.

Both simulations that include solar forcing (Fig. 1) show generally increasing temperatures through the twentieth century, with temperatures being about 1.5 K warmer by the end of the century than at the beginning. However the two series have rather different evolutions of temperature change; the 10×HS simulation shows two distinct periods of warming and a cooler period in

the 1960s and 1970s, whereas the 10×LBB simulation has a more gradual but consistent warming trend throughout the century. The plot of global-mean temperatures from the 5×VOL run clearly shows the cooling impact of Krakatoa and subsequent volcanoes in the late nineteenth and early twentieth centuries and cooling in the late twentieth century from the Agung, El Chichón, and Pinatubo eruptions. In between there is a period of warmer temperatures from 1920 to 1960. The observations show two distinct periods of warming, between circa 1910 and 1945 and after 1975. The reconstruction of Hoyt and Schatten (1993) is based on solar cycle length whereas the reconstruction of Lean et al. (1995a) is based on solar cycle amplitude; Friis-Christensen and Lassen (1991) noted that twentieth-century global temperatures changes correlated well with solar cycle length.

a. Test for linearity

In order to analyze simulations that include enhanced forcings, the large-scale response to enhanced forcings must scale linearly. We have checked this by regressing 10×LBB and 5×VOL against NATURAL, the latter containing the same solar and volcanic forcings that are enhanced in 10×LBB and 5×VOL by factors of 10 and 5, respectively. The same optimal detection procedure is followed as described above. If the large-scale response is linear, we would expect the scaling factors for 10×LBB and 5×VOL to be 0.1 and 0.2, respectively. At a truncation of 24, the best estimates of the 10×LBB and 5×VOL scaling factors are 0.12 and 0.18, respectively, with 5–95 percentile uncertainty ranges of 0.03–0.22 and 0.08–0.30. Values vary with the exact value of truncation chosen; taking the mean of the best estimates of the solar and volcanic scaling factors over all possible truncations gives 0.1 and 0.2. Therefore the climatic response to solar and volcanic forcings appears to scale linearly to the factors (10 and 5) used here, and we will henceforth calculate the scaling factors for LBB, HS, and VOL by multiplying the scaling factors for 10×LBB, 10×HS, and 5×VOL by 10, 10, and 5, respectively.

b. Decadal-mean attribution analysis

We now include the solar and volcanic runs in our analysis along with the anthropogenic runs in order to calculate the scaling factors, β_i , for four signals: G, SO, LBB, VOL. As for the analysis described in section 2, we extract the scaling factors for G, SO from a linear transformation of the GHG and ANTHRO scaling factors. As demonstrated in section 3a, the LBB and VOL scaling factors can be deduced from the 10×LBB and 5×VOL simulations. These are shown in Table 2 and refer to the model’s near-surface temperature response to unenhanced forcings.

We find that the scaling factor for LBB is estimated

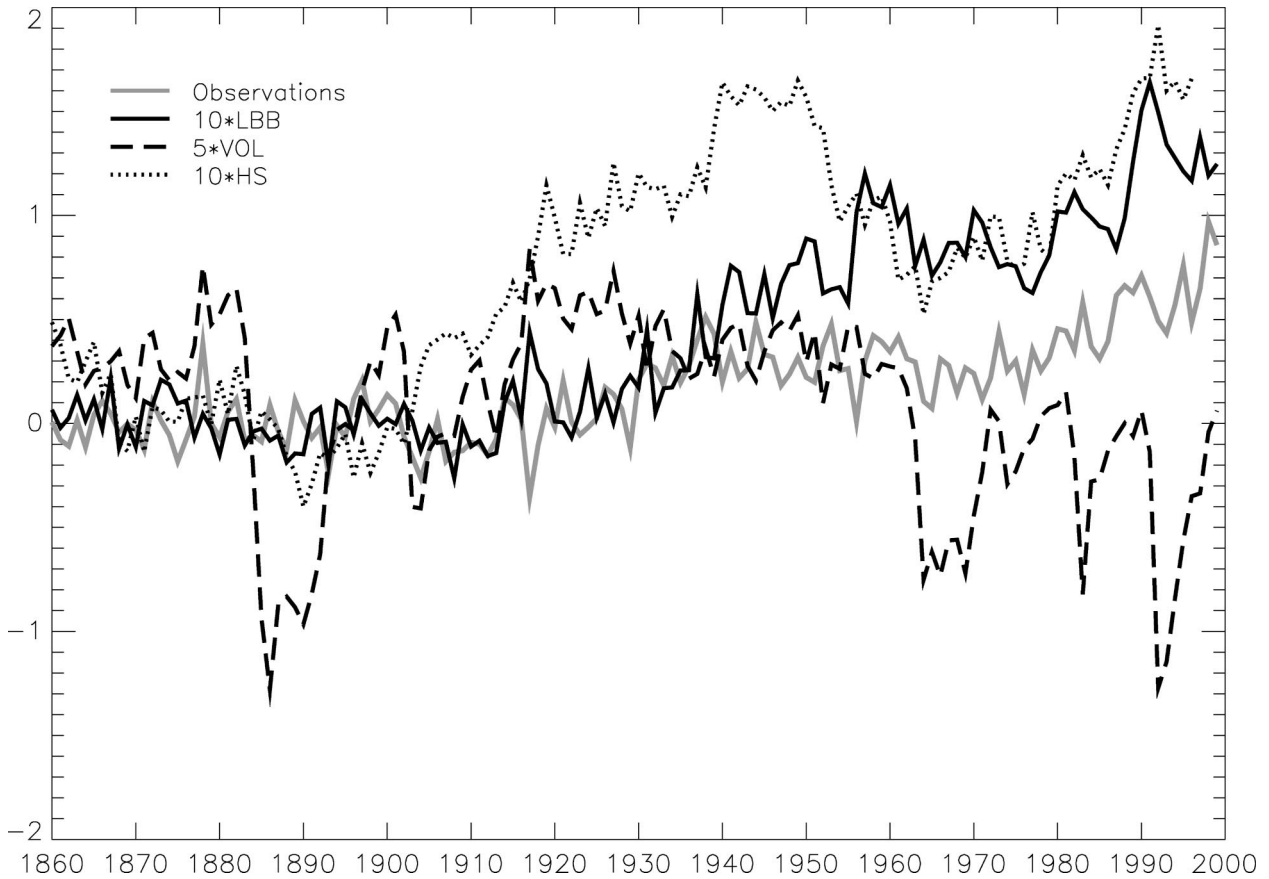


FIG. 1. Global-mean, annual-mean, near-surface temperatures expressed as anomalies with respect to the 1881–1920 mean for the $10 \times \text{LBB}$, $5 \times \text{VOL}$, and $10 \times \text{HS}$ simulations and the observations.

to be significantly greater than 1 (5th percentile greater than 1; Table 2, first row) and that for G to be significantly less than 1 (95th percentile less than 1, Table 2, first row). Scaling factors that are not consistent with 1 indicate that the model under- or overestimates the near-surface temperature response to the relevant forcing with values greater than 1 meaning that the model's response has to be amplified to agree with the observed response. These results imply that the model underestimates the solar contribution (since the model's response to solar forcing has to be amplified to be consistent with the observed response to solar forcing). The model also overestimates the greenhouse contribution (since the model's response to greenhouse forcing has to be downweighted to be consistent with the observed response), a finding that differs from the three-signal analysis shown in Table 1, in which solar and volcanic signals are constrained to have the same scalings, and in which the greenhouse scaling factor is consistent with 1.

To check these results, we replace the observations by ALL, the ensemble containing all the forcings included in the four separate ensembles. This ensemble has been shown by Stott et al. (2000) to successfully simulate many features of multidecadal global-mean and large-

scale land temperature variations during the twentieth century, although it fails to capture warming observed in the North Atlantic in the first half of the century.

Regressed against ALL, the scaling factors of the individual signals are expected to be consistent with 1, since ALL is simply the sum of the individual components. When G, SO, NATURAL are regressed against ALL we find that all scaling factors are consistent with 1 as expected (Table 1, third row). We have already shown in section 2a that NATURAL is a linear combination of the solar and volcanic components, because $10 \times \text{LBB}$ and $5 \times \text{VOL}$ regressed against NATURAL gave scaling factors consistent with 0.1 and 0.2 as expected. However when G, SO, $10 \times \text{LBB}$, and $5 \times \text{VOL}$ are regressed against ALL and recast into scaling factors, β_i , on G, SO, LBB, and VOL, we find that they are not all consistent with 1 (Table 2, second row). Instead the β for G is significantly less than 1. The LBB β is consistent with 1, although its uncertainty range is mostly greater than 1. Since the model's response to different forcings appears to add linearly, it seems likely that there is something in the nature of the combination of signals that would lead (in regression against the observations) to a significant, and erroneous, underes-

TABLE 2. Best estimates of scaling factors, β_i , for analyses of the 1900–99 period including separate solar and volcanic simulations (with the 5th–95th percentile range shown in parentheses).

	G	SO	LBB	VOL
10-yr means vs observations	0.49 (0.16–0.80)	0.81 (0.35–1.39)	3.88 (2.68–5.43)	0.54 (−0.19 to 1.18)
10-yr means vs ALL	0.59 (0.31–0.88)	0.59 (0.18–1.05)	2.07 (0.93–3.33)	1.00 (0.42–1.58)
5-yr means vs observations	0.81 (0.50–1.14)	1.01 (0.53–1.61)	2.64 (1.34–4.21)	0.39 (−0.13 to 1.01)
5-yr means vs ALL	0.74 (0.45–1.05)	0.81 (0.38–1.33)	1.92 (0.70–3.32)	0.86 (0.31–1.39)
	G	SO	HS	VOL
5-yr mean vs observations	0.60 (0.16–1.06)	0.46 (−0.01 to 0.97)	1.96 (0.77–3.14)	−0.14 (−0.83 to 0.52)

timate of the β for G and overestimate of the β for LBB. This could occur, for example, through degeneracy between signals. Thus although our results indicate that our model underestimates the observed response to solar forcing, some of this apparent underestimate could be an artifact of degeneracy between the greenhouse and solar signals.

c. The 5-yr mean attribution analysis

Increasing the temporal resolution of model signals enables the regression to better distinguish them, alleviating some of the problems associated with signal degeneracy, although it reduces the amount of spatial information that can be represented by the leading 24 spatiotemporal modes of variability. By using 5-yr rather than 10-yr means in the perfect model experiment in which G, SO, LBB, and VOL are regressed against ALL, the scaling factors for the four model signals are now all consistent with their expected values of 1 (Table 2, fourth row), although there are still indications that β values for G and SO are being systematically underestimated and the LBB β is being systematically overestimated. Regressed against the observations (Table 2, third row), the scaling factors are still consistent with 1 except that for the solar signal, which is estimated to be between 1.34 and 4.21 (5th and 95th percentiles) with a best estimate of 2.64. Including the model's response to the alternative solar reconstruction of Hoyt and Schatten (1993) in the regression, we find that the solar scaling factor is between 0.77 and 3.14 with a best estimate of 1.96. Therefore, whichever reconstruction is used, the large-scale temperature response to changes in solar output appears to be underestimated by the model.

This conclusion is consistent with other detection studies which have also found evidence that models could be underestimating the temperature response to solar forcing. Stott et al. (2003) found that the observed solar signal was likely to have been underestimated by the HadCM2 model when forced by the reconstruction of Hoyt and Schatten (1993). That study analyzed the same 50-yr periods as Tett et al. (1999) and found a very large uncertainty range for the scaling factors in the 1906–56 period, including unbounded values and a 5th percentile greater than 1, indicating that the real world's response to solar forcing could be greater than

that of the model's. Hill et al. (2001) detected the influence of solar forcing in changes in vertical temperature structure between 1961 and 1995 and found evidence that the HadCM2 GCM underestimated the observed response to solar forcing by a factor of 2–3. In addition, North and Wu (2001), purely investigating the 11-yr solar cycle component of solar variability, found evidence for models systematically underestimating the near-surface temperature response to solar irradiance changes by a factor of about 2.

d. Reconstructed anthropogenic and natural contributions to observed temperature changes

Figure 2 shows two alternative reconstructions of global-mean temperature changes over the twentieth century, attributed to the different climate forcings, depending on whether the LBB reconstruction or the HS reconstruction is included in the analysis. In both cases, there is a general warming trend during the century from greenhouse gases. Sulfate cooling is most important in the middle of the century, although there is some uncertainty as to the degree of cooling depending on which solar reconstruction is chosen. Volcanoes play a relatively minor role in our analyses although they are detected in annually resolved data (Stott et al. 2001). There are striking differences between the patterns of solar-induced temperature changes. There is a general warming trend from the LBB simulation with some cooling in the 1960s whereas the HS simulation shows a much more distinct warming peak in the 1940s (a solar cycle earlier than the much smaller peak in LBB) and a much larger late century warming trend following a dip in the 1960s. These differences are consistent with differences between the irradiance reconstructions.

According to our analysis, solar forcing is likely to be proportionately more important in the first half than the second half of the twentieth century. Reconstructed 50-yr trends for 1900–49 and 1950–99, and their uncertainties, are shown in Fig. 3 for the analysis including the LBB reconstruction of solar irradiance. Whereas in the 1950–99 period greenhouse warming dominates, in the 1900–49 period, the best estimate of solar warming ($0.29 \text{ K century}^{-1}$) is greater than the best estimate of greenhouse warming ($0.27 \text{ K century}^{-1}$).

Table 3 also includes trends estimated using the HS

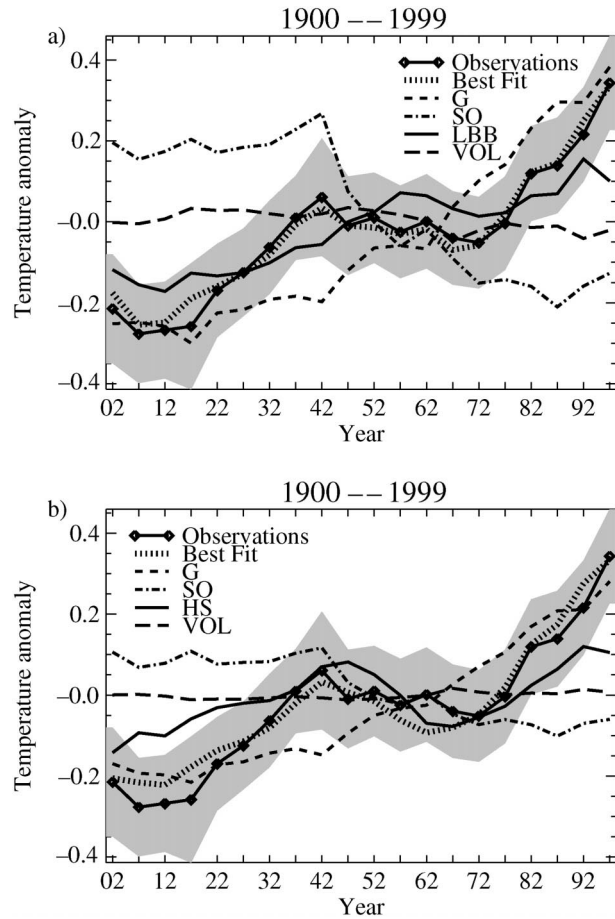


FIG. 2. Decadal-mean global-mean temperature changes over the twentieth century for (a) the observations (solid line) and the best-fit reconstructions estimated from regression [Eq. (2)] of the contributions from greenhouse gases (G), sulfate aerosols and ozone (SO), changes in solar irradiance according to the reconstruction of Lean et al. (1993) (LBB), and volcanic aerosol (VOL); and (b) the best-fit reconstructions of the combinations from G, SO, changes in solar irradiance according to the reconstruction of Hoyt and Schatten (1993; HS), and VOL.

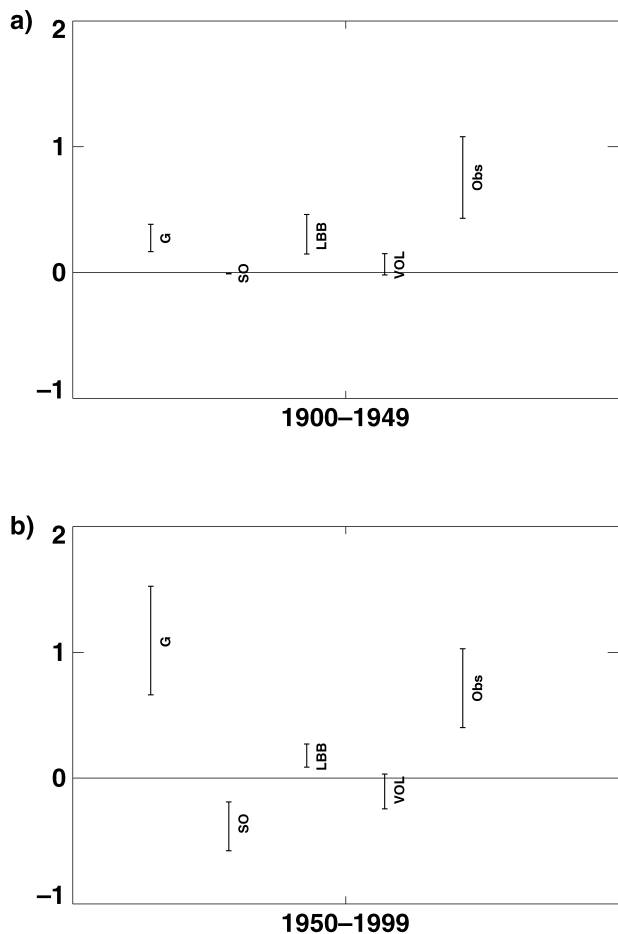


FIG. 3. Estimated trends in K century⁻¹ (5th–95th percentile uncertainty ranges) for G, SO, LBB, VOL for (a) 1900–50, (b) 1950–99.

reconstruction. For the 1900–49 period our best estimates are that increases in solar irradiance as reconstructed by Hoyt and Schatten (1993) caused over 60% of the warming and as reconstructed by Lean et al. (1995a) caused over 40% of the warming. In the second half of the century, the best estimate of the warming from greenhouse gas increases is a factor 2.75 or 6.35 greater than that from solar-induced warming using the

TABLE 3. Best estimates of the estimated trends in K century⁻¹ (with the 5th–95th percentile range shown in parentheses) using data averaged over 5-yr means.

	1900–99	1900–49	1950–99	1970–99
G	0.69 (0.42–0.97)	0.27 (0.17–0.38)	1.08 (0.66–1.53)	1.10 (0.67–1.55)
SO	-0.49 (-0.26 to -0.78)	-0.01 (-0.01 to 0.00)	-0.36 (-0.58 to -0.19)	0.01 (0.01–0.02)
LBB	0.31 (0.16–0.49)	0.29 (0.15–0.46)	0.17 (0.09–0.27)	0.48 (0.29–0.76)
VOL	-0.05 (-0.12 to 0.02)	0.06 (-0.02 to 0.15)	-0.10 (-0.24 to 0.03)	-0.06 (-0.15–0.02)
G	0.51 (0.14–0.91)	0.19 (0.05–0.33)	0.77 (0.21–1.36)	0.80 (0.22–1.43)
SO	-0.23 (-0.49 to 0.01)	-0.03 (-0.07 to 0.00)	-0.17 (-0.36 to 0.01)	0.01 (0.00–0.01)
HS	0.16 (0.06–0.25)	0.47 (0.19–0.75)	0.28 (0.11–0.45)	0.73 (0.29–1.17)
VOL	0.02 (-0.06 to 0.10)	-0.02 (-0.12 to 0.08)	0.03 (-0.12 to 0.20)	0.02 (-0.08 to 0.13)
Observations	0.49	0.76	0.72	1.52

Hoyt and Schatten (1993) and the Lean et al. (1995a) reconstruction, respectively. Whereas we estimate that greenhouse warming is likely to have caused more warming than observed during 1950–99, with greenhouse gas warming offset by cooling from sulfate aerosols, our best estimate is that warming from solar forcing is 16% and 36% of the greenhouse warming with the LBB and HS reconstructions, respectively.

Although scaling factors, β , for all four model signals (G, SO, LBB, VOL) are consistent with 1 when regressed against ALL (Table 2, fourth row), the probability that G has a scaling factor less than 1 remains high at 90%. A general tendency for G to be downweighted is also seen in regressions against the observations with best estimates of its scaling factors being 0.81 when regressed with LBB and 0.60 when regressed with HS (Table 2, third and fifth rows).

Degeneracy between G and HS is greater than that between G and LBB, as shown by both the greenhouse gas and solar contributions being less well constrained (Table 3) when HS rather than LBB is included in the regression. At the lower end of the large uncertainty range of the G scaling factor, the estimated greenhouse gas contribution to observed warming over the last 50 yr is less than the best-fit HS solar contribution. However, whereas there is a 12% probability that HS solar warming exceeds greenhouse warming (consistent with a 5th percentile of the G scaling factor of only 0.16), there is only a 0.2% probability that LBB solar warming exceeds greenhouse warming. Solar forcing is estimated to have made a larger relative contribution to warming during the last three decades of the twentieth century than during the last five decades (Table 3). For both HS and LBB the greenhouse contribution is downweighted (best estimates of the scaling factors less than 1 in the third and fifth rows of Table 2) and, as was discussed in section 3c, it seems likely that our methodology erroneously overestimates the solar component and underestimates the greenhouse component of observed warming, as a result of degeneracy between the patterns of response to these two forcings. Therefore the trends attributed to solar forcing in Table 3 are likely to be an overestimate.

Amplifying the solar signal, in combination with the anthropogenic and volcanic signals, produces an improved fit to the observed large-scale temperature evolution during the twentieth century. Global warming observed over the last three decades is well reproduced by the ANTHRO ensemble alone but the addition of an enhanced solar contribution improves the fit to early century warming. However, despite the improved fit to global-mean temperatures, Fig. 4 shows that the spatial pattern of early century warming in the North Atlantic is not well simulated, even with the addition of more solar-induced warming. The ALL ensemble also fails to capture the observed warming in the North Atlantic (Stott et al. 2000). The observed warming in this region cannot be accounted for by the external forcings in-

cluded thus far, but variations in the Atlantic thermohaline circulation could account for such a pattern of warming. Delworth and Knutson (2000) showed that one simulation, whose thermohaline circulation happened to strengthen in an ensemble of anthropogenically forced simulations, captured the early century warming.

Our results show a large contribution of solar forcing to early century warming. It is possible however that some of this solar warming could be a spurious attempt by the regression scheme to fit global-mean warming in the first half of the twentieth century caused by changes in the thermohaline circulation in the North Atlantic. When the North Atlantic region (ocean grid points between 0° – 90° N and 90° W– 0°) is masked out and the analysis is repeated we find that solar scaling factors are reduced somewhat (best estimates are reduced from 2.64 to 1.91 for LBB and from 1.96 to 1.71 for HS). Thus, the apparent enhanced climatic response to solar forcing remains in the observations, and cannot be explained by the regression scheme overfitting the solar response to observed early century warming in the North Atlantic.

4. Summary and discussion

Previous optimal detection analyses that compared twentieth-century model-simulated climate change signals with observed changes in near-surface temperature have found that late twentieth-century warming was almost entirely caused by increases in greenhouse gases. However these calculations relied on a methodology whose systematic bias results in an underestimate of the climatic response attributed to weak climate change signals subject to sampling noise. Therefore previous results could have overestimated the observed warming attributed to anthropogenic factors and underestimated the observed warming attributed to natural factors.

We have made two simulations including solar forcing, using two alternative reconstructions of solar irradiance variation, and a simulation including volcanic forcing. In all these simulations the forcings have been enhanced to increase the signal strength, by a factor of 10 in the case of the solar simulations and by a factor of 5 in the case of the volcanic simulation. We have shown that linearity allows us to estimate the observed response to the nonenhanced forcings by a simple scaling. In addition we have used an improved form of optimal fingerprinting that takes account of sampling noise in model-simulated signals. Our results imply that solar forcing had a greater impact on near-surface temperatures than simulated by HadCM3, and that previous attribution analyses may have underestimated the potential contribution of solar forcing to twentieth-century global warming. We find that climatic processes could act to amplify the near-surface temperature response to (non enhanced) solar forcing by between 1.34 and 4.21 for LBB and 0.70 to 3.32 for HS, although degeneracy between the greenhouse and solar signals (especially

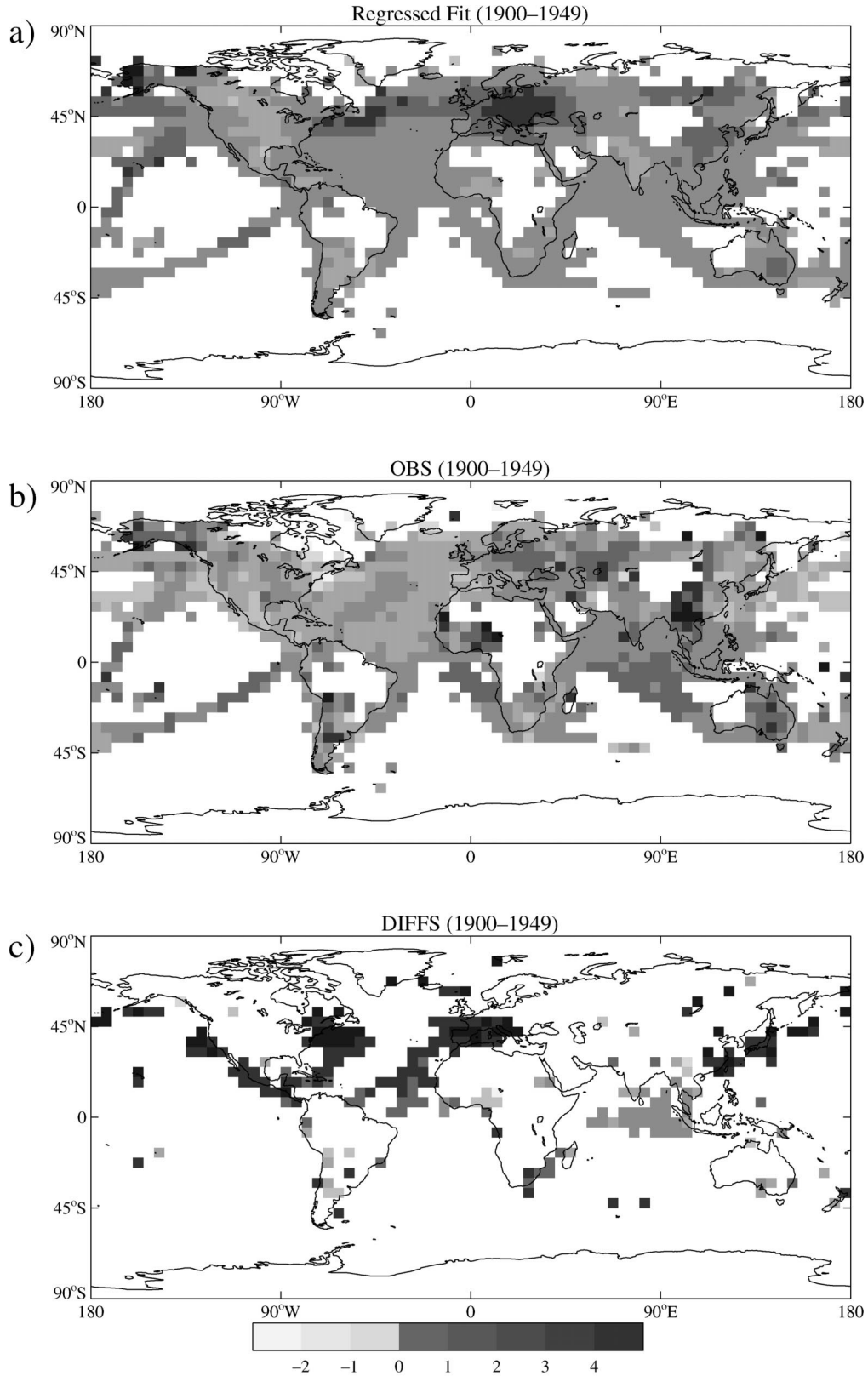


FIG. 4. Near-surface temperature trends (K century^{-1}) for the 1900–49 period for (a) modeled trend obtained by regressed fit to the observations including contributions from G, SO, LBB, VOL; (b) observed trend; (c) differences significant at the $p = 0.1$ level according to a two-sided t test.

HS—see earlier in this paper) could spuriously increase this upper limit.

Even with such an enhanced climate response to solar forcing, most warming over the last 50 yr is likely to have been caused by increases in greenhouse gases. Indeed we estimate that increases in greenhouse gases were likely to have caused more warming than observed, with a significant cooling trend from the direct and indirect effects of sulfate aerosols counterbalancing the combined warming effects from greenhouse gases and changes in solar irradiance. The best estimate of the warming from solar forcing is estimated to be 16% or 36% of greenhouse warming depending on the solar reconstruction.

Any potential amplification of solar forcing by the climate system would increase the potential climatic impact of future changes in solar irradiance. Lean (2001) has estimated that forcing due to changes in total solar irradiance between the solar cycle minima in 1996 and 2016 is likely to be in the range of $\pm 0.1 \text{ W m}^{-2}$ in comparison with the net anthropogenic climate forcing over the 22-yr period of 0.5 to 0.9 W m^{-2} , where she has based her estimates on past records of multidecadal-scale solar variability. An enhancement of the solar forcing by a factor of 3 would therefore increase the potential future solar forcing to $\pm 0.3 \text{ W m}^{-2}$, the upper limit of which is more than half the lower limit of anthropogenic forcing. A reduction of the greenhouse gas contribution to 81% of its modeled value (the best estimate of the scaling factor for G in combination with LBB; Table 2), while keeping the aerosol contribution approximately the same [the best estimate of the scaling factor for S being 1.01, Table 2; note that the relative proportions of greenhouse gas and sulfur emissions change during the course of the different IPCC Special Report on Emissions Scenarios (SRES) scenarios] would result in a reduction of anthropogenic global warming forecast under the IPCC SRES scenarios (Nakicenovic and Swart 2000; Houghton et al. 2001) of 0.15 K by the mid-2020s (from 0.6 K relative to the 1990s) and between 0.3 K for the B1 scenario by the 2090s (from 1.8 K relative to the 1990s) and 0.7 K for the A1FI scenario by the 2090s (from 4.1 K).

The results presented here indicate the potential importance of solar forcing. However some important caveats should be kept in mind. Reconstructions of solar irradiance are empirically based and are very uncertain, reconstructions differing due to the various assumptions used. Despite the improvement to the modeled fit of global-mean temperatures gained by enhancing solar-induced changes, there is no improvement in the simulation of North Atlantic warming during the first half of the century. This warming may be associated with a multidecadal-scale mode of variability or a forcing missing from the model.

Reducing the data-averaging period from 10 to 5 yr helps distinguish different fingerprints by reducing their degeneracy. However, degeneracy between patterns of

response to greenhouse gases and solar forcing, particularly HS, means that the relative contributions of these two forcings to recent global warming are poorly constrained. When regressed in perfect model experiments against ALL we find that the scaling factors for all signals are consistent with the expected values of 1 although there is a tendency for downweighting of the greenhouse gas and upweighting of the solar contributions, indicating that we could have overestimated the solar contribution and underestimated the greenhouse gas contribution to observed warming.

Nevertheless, our main conclusion, that models underestimate the climatic response to solar forcing, is supported by two other detection studies that used diagnostics tailored for the 11-yr solar cycle. Hill et al. (2001) showed that models underestimate the tropospheric temperature response to solar forcing by a factor of 2 to 3 and North and Wu (2001) found an underestimate of about 2 for near-surface temperatures.

These results indicate that climatic processes, not present in the model, have acted to alter the magnitude of the large-scale spatial and temporal near-surface temperature response. Our methodology is not designed to identify missing processes that alter small-scale details of the response. Although our study indicates that there could be an enhanced global-scale temperature response to solar forcing, convincing evidence for a mechanism remains elusive. Potentially the largest amplification of solar forcing could result from modulation of stratospheric ozone by variations in solar ultraviolet, which could influence the troposphere via modulation of planetary waves (Shindell et al. 1999b) or modulation of the Hadley circulation (Haigh 1996), although none of the published studies indicate that ozone feedback could enhance solar radiative forcing by more than a factor of one-half (J. D. Haigh 2003, personal communication). Alternatively, solar effects on climate could be mediated by cosmic rays, the intensity of which has declined at the earth as the interplanetary magnetic field increased during the twentieth century. It has been speculated that cosmic rays could modulate global temperature by changing clouds (Marsh and Svensmark 2000; Yu 2002) or by altering the global electric circuit (Harrison 2002). The results presented here suggest that climate models underestimate the sensitivity of the climate system to changes in solar irradiance, but a conclusive demonstration of an enhanced role for solar forcing requires an understanding of the physical mechanisms underlying such an effect.

Acknowledgments. This work was funded by the U.K. Department for Environment, Food and Rural Affairs under contract PECD 7/12/37 (PAS, GSJ) and the U.K. Government Meteorological Research and Development Programme (JFBM). We thank the reviewers for their helpful comments.

APPENDIX A

Details of HadCM3 Simulations

Further details of the forcings included in the HadCM3 simulations analyzed in this paper are given below and are outlined in more detail in Tett et al. (2002).

a. Well-mixed greenhouse gases

Runs forced with the well-mixed greenhouse gases CO₂, CH₄, N₂O, and six CFCs/HCFCs use historical values before 1990 (Schimel et al. 1996) and from 1990 values from the preliminary B2 IPCC SRES scenario. Johns et al. (2003) describe how emissions of greenhouse gases were converted to concentrations.

b. Sulfates

The direct effect of sulfate aerosols on planetary albedo was simulated using a fully interactive sulfur cycle scheme that models the emission, transport, oxidation, and removal of sulfur species. Estimates of the anthropogenic SO₂ emissions were taken from Orn et al. (1996) for 1860–1970, the Global Emissions Inventory Activity (GEIA) 1B dataset for 1985, and the preliminary SRES datasets for 1990 and 2000 (Nakićenović and Swart 2000) and linearly interpolated between these times. The distribution of atmospheric sulfate aerosol was then passed to the model's radiation scheme (Edwards and Slingo 1996; Cusack et al. 1999) for computation of its direct radiative effect.

The indirect effect of tropospheric aerosol on cloud reflectivity (Twomey 1974) was also represented in the model. This was computed using offline simulations of a modified version of HadAM3 (the atmospheric component of HadCM3) in which the aerosol distributions change the three-dimensional distribution of cloud albedo by affecting the cloud droplet concentrations seen by the radiation scheme. The change in cloud albedo calculated from the offline simulations is used to modify the cloud albedos in the HadCM3 coupled runs so as to simulate the indirect effect.

A further discussion of the validity of this approach is given by Tett et al. (2002). More details on the parameterization of the direct and indirect effects of sulfates in HadCM3 can be found in Johns et al. (2003).

c. Tropospheric ozone

Three-dimensional fields of monthly mean tropospheric ozone were computed using the STOCHEM chemical model (Collins et al. 1997) for 1860, 1900, 1950, 1975, 1990, and 2000. Values of ozone between those years were interpolated by assuming linearity between increases in observed methane concentration and modeled tropospheric ozone for each month in the year.

d. Stratospheric ozone

Stratospheric ozone depletion is included in the model by adding the seasonally and zonally varying trends in stratospheric ozone from Randel and Wu (1999) after 1979. From 1975 to 1979 half these trends were added to the annual cycle of preindustrial ozone above the diagnosed mean model-diagnosed tropopause.

e. Volcanic aerosol

Stratospheric volcanic aerosols are input to the model as quarterspheric values (in four latitude bands 90°–45°S, 45°S–0°, 0°–45°N, 45°–90°N) of monthly optical depths at 0.55 μm on using the updated time series of Sato et al. (1993) distributed above the model tropopause assuming a uniform mass mixing ratio.

f. Solar irradiance changes

Changes in solar irradiance, as estimated by Lean et al. (1995a) and by Hoyt and Schatten (1993) were applied to the model by varying the solar constant in the model's radiation scheme with the changes spread over the solar spectrum following Lean et al. (1995b), with a greater variation in solar ultraviolet (UV) than total irradiance.

APPENDIX B

Optimal Detection Procedure

The TLS regression model, Eq. (2), assumes uncertainty in both the observations, \mathbf{y} , and the model-simulated response patterns \mathbf{x}_i . The climate noise covariance,

$$\mathbf{C}_N \equiv \mathbb{E}(\mathbf{u}\mathbf{u}^T), \quad (B1)$$

\mathbb{E} being the expectation operator, is generally unknown and must be estimated from a control run of a climate model or from intraensemble differences. The noise is generally far from white, ie $\mathbf{C}_N \neq \sigma^2 \mathbf{I}$, and accurate estimates of β_i require a prewhitening operator, \mathbf{P} , to be introduced such that

$$\mathbb{E}(\mathbf{P}\mathbf{u}_i\mathbf{u}_i^T\mathbf{P}^T) = \mathbf{I}_\kappa \quad \text{and} \quad (B2)$$

$$\mathbb{E}(\mathbf{P}\mathbf{u}_0\mathbf{u}_0^T\mathbf{P}^T) = \mathbf{I}_\kappa, \quad (B3)$$

where \mathbf{I}_κ is the rank- κ unit matrix.

Here the assumption is made that the noise has the same autocorrelation structure in \mathbf{y} as in each \mathbf{x}_i . If this is not the case, for example if ensemble means have been used to reduce noise in model-simulated response patterns, the relevant \mathbf{x}_i can simply be scaled up to make the expected noise variance the same as that in \mathbf{y} , and the same scaling factor(s) applied to the final parameter estimates. See Allen and Stott (2003) for an expanded discussion of this point.

We define \mathbf{X} as the matrix whose m columns are the

model-simulated response patterns, \mathbf{x}_i , and we also define the $m' \times \kappa$ matrix (where $m' \equiv m + 1$)

$$\mathbf{Z} = [\mathbf{P}\mathbf{X}, \mathbf{P}\mathbf{y}], \quad (\text{B4})$$

as the observed (prewhitened but still noise contaminated) values of \mathbf{X} and \mathbf{y} .

Our basic linear model asserts that there exists a \mathbf{Z}^{true} whose columns are linearly related, that is,

$$\mathbf{Z}^{\text{true}}\mathbf{v} = (\mathbf{Z} - \mathbf{Y})\mathbf{v} = 0, \quad (\text{B5})$$

where \mathbf{v} is a rank- m' vector of coefficients, and \mathbf{Y} is an $m' \times \kappa$ matrix representing the true (prewhitened) noise contamination in the m' variables. All the elements of \mathbf{Y} are normally distributed with unit variance, so the maximum likelihood estimator of \mathbf{v} , $\tilde{\mathbf{v}}$, is given by maximizing

$$L = \text{constant} - \frac{1}{2}\text{tr}(\tilde{\mathbf{Y}}^T\tilde{\mathbf{Y}}), \quad (\text{B6})$$

where $\tilde{\mathbf{Y}} = \mathbf{Z} - \tilde{\mathbf{Z}}$ and $\tilde{\mathbf{Z}}\tilde{\mathbf{v}} = 0$. The rows of $\tilde{\mathbf{Y}}$ are uncorrelated with $\tilde{\mathbf{v}}$, so maximizing L is equivalent to minimizing the merit function:

$$s^2 = \tilde{\mathbf{v}}^T\tilde{\mathbf{Y}}^T\tilde{\mathbf{Y}}\tilde{\mathbf{v}}. \quad (\text{B7})$$

Incorporating the normalization constraint that $\tilde{\mathbf{v}}^T\tilde{\mathbf{v}} = 1$ into our merit function gives

$$s^2(\tilde{\mathbf{v}}) = \tilde{\mathbf{v}}^T\mathbf{Z}^T\mathbf{Z}\tilde{\mathbf{v}} + \lambda^2(1 - \tilde{\mathbf{v}}^T\tilde{\mathbf{v}}), \quad (\text{B8})$$

where λ^2 is a Lagrange multiplier. In geometric terms, minimizing s^2 is equivalent to finding the m -dimensional plane in an m' -dimensional space that minimizes the sum-squared perpendicular distance from the plane to the κ points defined by the rows of \mathbf{Z} .

Differentiation of (B8) with respect to $\tilde{\mathbf{v}}$ gives an eigenequation defining the stationary points of s^2 at which

$$\frac{1}{2} \frac{\partial(s^2)}{\partial(\tilde{\mathbf{v}})} = \mathbf{Z}^T\mathbf{Z}\tilde{\mathbf{v}} - \lambda^2\tilde{\mathbf{v}} = 0. \quad (\text{B9})$$

The solution that minimizes s^2 is $\lambda^2 = \lambda_{\min}^2$, the smallest eigenvalue of $\mathbf{Z}^T\mathbf{Z}$, and $\tilde{\mathbf{v}}$ being the corresponding eigenvector (the vector normal to the best-fit m -dimensional plane). In a practical implementation, we simply take the singular value decomposition (SVD) $\mathbf{Z} = \mathbf{U}\Lambda\mathbf{V}^T$ so, after sorting, $\tilde{\mathbf{v}} = \mathbf{v}_{m'}$.

The m' th element of the solution vector corresponds to the best-fit scaling parameter on the observations, \mathbf{y} , and since we require a model that reproduces the observations themselves rather than a scaled version thereof, we translate the coefficients of $\tilde{\mathbf{v}}$ into the scaling factors, β_i , of Eq. (2) by taking the ratios $\beta_i = [\tilde{\mathbf{v}}]_i / [\tilde{\mathbf{v}}]_{m'}$.

The methodology for calculating uncertainty in $\tilde{\beta}$ is described by Allen and Stott (2003). The estimates of the noise properties are uncertain; although ignoring these simplifies the analysis it can lead to “artificial skill,” that is, a systematic underestimation of the un-

certainties. The standard methodology for dealing with this problem is to base the uncertainty analysis on a set of noise realizations, $\hat{\mathbf{Y}}_2$, which are statistically independent from the set of noise realizations, $\hat{\mathbf{Y}}_1$, used to estimate \mathbf{P} . In the analyses described here, intraensemble variability from differences between members of the GHG, ANTHRO, NATURAL, and ALL ensembles and their respective ensemble means is used for estimating \mathbf{P} , that is, optimization. A 1830-yr segment of the control run is used to estimate $\hat{\mathbf{Y}}_2$, that is, for the uncertainty analysis. We estimate the number of degrees of freedom [in an identical manner to that described in section 4.2 of Tett et al. (2002)] of the intraensemble variability used for optimization to be 24 and we therefore truncate the analysis to the first 24 spatiotemporal modes of variability.

APPENDIX C

Linear Transformation of Scaling Factors

Assuming that the climate response to well-mixed greenhouse gases (\mathbf{x}_G) and the non-well-mixed greenhouse gas component (\mathbf{x}_{SO}) is linearly additive (Haywood et al. 1997), we can extract the latter component from the GHG and ANTHRO runs by

$$\mathbf{x}_{\text{ANTHRO}} = \mathbf{x}_G + \mathbf{x}_{SO}, \quad \mathbf{x}_{\text{GHG}} = \mathbf{x}_G. \quad (\text{C1})$$

The scaling factors of G and SO can then be calculated from

$$\begin{aligned} & \beta_{\text{GHG}}\mathbf{x}_{\text{GHG}} + \beta_{\text{ANTHRO}}\mathbf{x}_{\text{ANTHRO}} \\ &= \beta_{\text{GHG}}\mathbf{x}_G + \beta_{\text{ANTHRO}}(\mathbf{x}_G + \mathbf{x}_{SO}) \\ &= (\beta_{\text{GHG}} + \beta_{\text{ANTHRO}})\mathbf{x}_G + \beta_{\text{ANTHRO}}\mathbf{x}_{SO}. \end{aligned} \quad (\text{C2})$$

Thus, $\beta_G = \beta_{\text{GHG}} + \beta_{\text{ANTHRO}}$ and $\beta_{SO} = \beta_{\text{ANTHRO}}$, where β_G is our best estimate of the pure greenhouse effect. This may seem counterintuitive, but consider the case when ANTHRO perfectly describes the real world: now $\beta_{\text{GHG}} = 0$, $\beta_{\text{ANTHRO}} = 1$ and both G and SO have unit scaling factors.

REFERENCES

- Allen, M. R., and S. F. B. Tett, 1999: Checking for model consistency in optimal fingerprinting. *Climate Dyn.*, **15**, 419–434.
- , and P. A. Stott, 2003: Estimating signal amplitudes in optimal fingerprinting. Part I: Theory. *Climate Dyn.*, doi:10.1007/s00382-003-0313-9.
- , —, J. F. B. Mitchell, R. Schnur, and T. L. Delworth, 2000: Uncertainty in forecasts of anthropogenic climate change. *Nature*, **407**, 617–620.
- , —, and Coauthors, 2002: Quantifying anthropogenic influence on recent near-surface temperature change. *Surv. Geophys.*, in press.
- Barnett, T. P. K., and Coauthors, 1999: Detection and attribution of climate change: A status report. *Bull. Amer. Meteor. Soc.*, **80**, 2631–2659.
- Carslaw, K. S., R. G. Harrison, and J. Kirkby, 2002: Cosmic rays, clouds and climate. *Science*, **298**, 1732–1737.
- Collins, W. J., D. S. Stevenson, C. E. Johnson, and R. G. Derwent, 1997: Tropospheric ozone in a global-scale three-dimensional

- Lagrangian model and its response to NO_x emission controls. *J. Atmos. Chem.*, **26**, 223–274.
- Crowley, T. J., 2000: Causes of climate change over the past 1000 years. *Science*, **289**, 270–277.
- Cubasch, U., R. Voss, G. C. Hegerl, J. Waszkewitz, and T. Crowley, 1997: Simulation of the influence of solar radiation variations on the global climate with an ocean-atmosphere general circulation model. *Climate Dyn.*, **13**, 757–767.
- Cusack, S., J. M. Edwards, and J. M. Crowley, 1999: Investigating k distribution methods for parameterizing gaseous absorption in the Hadley Centre climate model. *J. Geophys. Res.*, **104**, 2051–2057.
- Dai, A., T. M. L. Wigley, B. A. Boville, J. T. Kiehl, and L. E. Buja, 2001: Climates of the twentieth and twenty-first centuries simulated by the NCAR climate system model. *J. Climate*, **14**, 485–519.
- Delworth, T. L., and T. R. Knutson, 2000: Simulation of early 20th century global warming. *Science*, **287**, 2246–2250.
- Edwards, J. M., and A. Slingo, 1996: Studies with a flexible new radiation code. I: Choosing a configuration for a large-scale model. *Quart. J. Roy. Meteor. Soc.*, **122**, 689–719.
- Friis-Christensen, E., and K. Lassen, 1991: Length of the solar cycle: An indicator of solar activity closely associated with climate. *Science*, **254**, 698–700.
- Gillett, N. P., M. R. Allen, and K. D. Williams, 2002: The role of stratospheric resolution in simulating the Arctic oscillation response to greenhouse gases. *Geophys. Res. Lett.*, **29**, 1500, doi:10.1029/2001GL014444.
- Gordon, C., C. Cooper, H. Banks, J. M. Gregory, T. C. Johns, J. F. B. Mitchell, and R. A. Wood, 2000: The simulation of SST, sea ice extents and ocean heat transports in a version of the Hadley Centre coupled model without flux adjustments. *Climate Dyn.*, **16**, 147–168.
- Haigh, J. D., 1996: Impact of solar variability on climate. *Science*, **272**, 981–984.
- Harrison, R. G., 2002: Twentieth century secular decreases in the atmospheric potential gradient. *Geophys. Res. Lett.*, **29**, 1660, doi:10.1029/2002GL014878.
- Hasselmann, K., 1993: Optimal fingerprints for the detection of time-dependent climate change. *J. Climate*, **6**, 1957–1971.
- Haywood, J. M., R. J. Stouffer, R. T. Wetherald, S. Manabe, and V. Ramaswamy, 1997: Transient response of a coupled model to estimated changes in greenhouse gas and sulfate concentrations. *Geophys. Res. Lett.*, **24**, 1335–1338.
- Hegerl, G. C., T. J. Crowley, S. K. Baum, K.-Y. Kim, and W. T. Hyde, 2003: Detection of volcanic, solar and greenhouse gas signals in paleoclimate data. *Geophys. Res. Lett.*, **30**, 1242, doi:10.1029/2002GL016635.
- Hill, D. C., M. R. Allen, N. P. Gillett, S. F. B. Tett, P. A. Stott, G. S. Jones, W. J. Ingram, and J. F. B. Mitchell, 2001: Natural and anthropogenic causes of recent climate change. *Detecting and Modelling Regional Climate Change*, M. B. India and D. L. Bonillo, Eds., Springer-Verlag, 275–290.
- Houghton, J. T., Y. Ding, D. J. Griggs, M. Noguer, P. J. van der Linden, and D. Xiaosu, Eds., 2001: *Climate Change 2001: The Scientific Basis*. Cambridge University Press, 881 pp.
- Hoyt, D. V., and K. H. Schatten, 1993: A discussion of plausible solar irradiance variations, 1700–1992. *J. Geophys. Res.*, **98**, 18 895–18 906.
- Johns, T. C., and Coauthors, 2003: Anthropogenic climate change for 1860 to 2100 simulated with the HadCM3 model under updated emissions scenarios. *Climate Dyn.*, **20**, 583–612.
- Larkin, A., H. High, and S. Djavidnia, 2000: The effect of solar uv irradiance variations on the earth's atmosphere. *Space Sci. Rev.*, **94**, 199–214.
- Lean, J., 2000: Evolution of the sun's spectral irradiance since the Maunder Minimum. *Geophys. Res. Lett.*, **27**, 2425–2428.
- , 2001: Solar irradiance and climate forcing in the near future. *Geophys. Res. Lett.*, **28**, 4119–4122.
- , J. Beer, and R. Bradley, 1995a: Reconstruction of solar irradiance since 1610: Implications for climate change. *Geophys. Res. Lett.*, **22**, 3195–3198.
- , O. R. White, and A. Skumanich, 1995b: On the solar ultraviolet spectral irradiance during the mauer minimum. *Global Biogeochem. Cycles*, **9**, 171–182.
- , Y.-M. Wang, and N. R. Sheeley Jr., 2002: The effect of increasing solar activity on the sun's total and open magnetic flux during multiple cycles: Implications for solar forcing of climate. *Geophys. Res. Lett.*, **29**, 2224, doi:10.1029/2002GL015880.
- Lockwood, M., R. Stamper, and M. N. Wild, 1999: A doubling of the sun's coronal magnetic field during the past 100 years. *Nature*, **399**, 437–439.
- Marsh, N., and H. Svensmark, 2000: Low cloud properties influenced by cosmic rays. *Phys. Rev. Lett.*, **85**, 5004–5007.
- Mitchell, J. F. B., D. J. Karoly, G. C. Hegerl, F. W. Zwiers, M. R. Allen, and J. Marengo, 2001: Detection of climate change and attribution of causes. *Climate Change 2001: The Scientific Basis*, J. T. Houghton et al., Eds., Cambridge University Press, 695–738.
- Nakićenović, N., and R. Swart, Eds., 2000: *Special Report on Emission Scenarios*. Cambridge University Press, 570 pp.
- North, G. R., and Q. Wu, 2001: Detecting climate signals using space-time EOFs. *J. Climate*, **14**, 1839–1863.
- Orn, G., U. Hansson, and H. Rodhe, 1996: Historical worldwide emissions of anthropogenic sulfur: 1860–1985. Department of Meteorology/International Meteorological Institute, Stockholm University, Tech. Rep. CM-91, 5 pp. and 15 plates.
- Parker, D. E., P. D. Jones, C. K. Folland, and A. Bevan, 1994: Interdecadal changes of surface temperature since the late nineteenth century. *J. Geophys. Res.*, **99**, 14 373–14 399.
- Pope, V. D., M. L. Gallani, P. R. Rowntree, and R. A. Stratton, 2000: The impact of new physical parameterizations in the Hadley Centre climate model—HadAM3. *Climate Dyn.*, **16**, 123–146.
- Randel, W. J., and F. Wu, 1999: A stratospheric ozone trends data set for global modelling studies. *Geophys. Res. Lett.*, **26**, 3089–3092.
- Rind, D., 2002: The sun's role in climate variability. *Science*, **296**, 673–677.
- Ripley, B. D., and M. Thompson, 1987: Regression techniques for the detection of an analytical bias. *Analyst*, **112**, 377–383.
- Sato, M., J. E. Hansen, M. P. McCormick, and J. B. Pollack, 1993: Stratospheric aerosol optical depths (1850–1990). *J. Geophys. Res.*, **98**, 22 987–22 994.
- Schimel, D., and Coauthors, 1996: Radiative forcing of climate change. *Climate Change 1995: The Science of Climate Change*, J. T. Houghton, et al., Eds., Cambridge University Press, 65–131.
- Shindell, D. T., R. L. Miller, G. A. Schmidt, and L. Pandolfo, 1999a: Simulation of recent northern winter climate trends by greenhouse-gas forcing. *Nature*, **399**, 452–455.
- , D. Rind, N. Balachandran, J. Lean, and P. Lonergan, 1999b: Solar cycle variability, ozone and climate. *Science*, **284**, 305–308.
- Solanki, S. K., and M. Fligge, 2002: Solar irradiance variations and climate. *J. Atmos. Solar Terr. Phys.*, **64**, 677–685.
- Stott, P. A., and S. F. B. Tett, 1998: Scale-dependent detection of climate change. *J. Climate*, **11**, 3282–3294.
- , and J. A. Kettleborough, 2002: Origins and estimates of uncertainty in predictions of twenty first century temperature rise. *Nature*, **416**, 723–726.
- , S. F. B. Tett, G. S. Jones, M. R. Allen, J. F. B. Mitchell, and G. J. Jenkins, 2000: External control of 20th century temperature by natural and anthropogenic forcings. *Science*, **290**, 2133–2137.
- , —, —, —, W. J. Ingram, and J. F. B. Mitchell, 2001: Attribution of twentieth century temperature change to natural and anthropogenic causes. *Climate Dyn.*, **17**, 1–21.
- , M. R. Allen, and G. S. Jones, 2003: Estimating signal ampli-

- tudes in optimal fingerprinting. Part II: Application to general-circulation models. *Climate Dyn.*, doi:10.1007/s00382-003-0314-8.
- Tett, S. F. B., P. A. Stott, M. R. Allen, W. J. Ingram, and J. F. B. Mitchell, 1999: Causes of twentieth century temperature change near the earth's surface. *Nature*, **399**, 569–572.
- , and Coauthors, 2002: Estimation of natural and anthropogenic contributions to 20th century temperature change. *J. Geophys. Res.*, **107**, 4306, doi:10.1029/2000JD000028.
- Twomey, S. A., 1974: Pollution and the planetary albedo. *Atmos. Environ.*, **8**, 1251–1256.
- Yu, F., 2002: Altitude variations of cosmic ray induced production of aerosols: Implications for global cloudiness and climate. *J. Geophys. Res.*, **107**, 1118, doi:10.1029/2001JA000248.